

# Steering SuperDARN Radars

by

Raymond A. Greenwald  
ECE, Virginia Tech

## Introduction

An important capability for making observations with any radar is the ability to form a well-defined radar beam and steer that beam into a variety of viewing directions. Over the past 30-40 years the focus of this effort has gone in the direction of electronic steering using one or two dimensional arrays of antennas. If we assume a one-dimensional array of antennas each of which has a common viewing direction, then the radiation pattern of this array is determined by the product of the radiation pattern due to the individual antennas and the interference pattern of an array of isotropic radiators that are located at the location of each of the antennas in the array. The directions of the maxima of this interference pattern are, of course, dependent on the phase shift in the transmitted signals between adjacent pairs of antennas. If there is no phase shift, then the peak in the interference pattern is normal to the line of antenna array and, if we assume that the antennas are radiating horizontally, then the composite pattern of  $N$  antennas would be a vertical fan-shaped beam. The vertical shape of the pattern would be the same as that due to a single radiating element over a ground plane,. It is unaffected by the number of elements in the array. In contrast, the horizontal shape of the pattern is strongly impacted by the number of antennas, since the signals from the antennas must be summed. Assuming the antennas to be horizontally polarized the total horizontal electric field from an array of  $N$  antennas is given by

$$E = \frac{\sin(\pi(N-1)d\sin(\theta)/\lambda)}{\pi(N-1)d\sin(\theta)/\lambda} \quad (1)$$

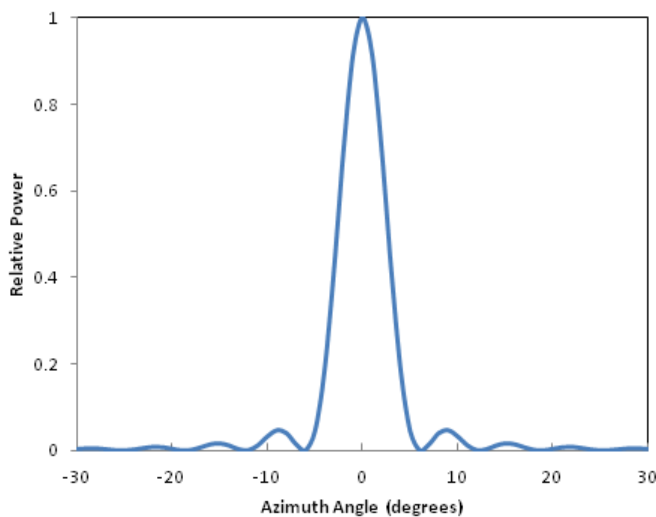


Figure 1.

If we consider typical operating parameters for the primary array of a SuperDARN radar, e.g.  $N=16$ ,  $d=15.24\text{m}$  (antenna separation), and  $\lambda=24\text{m}$  (wavelength for a radar transmission frequency of 12.5 MHz), the radiated power density as a function of the azimuth angle  $\theta$  is proportional to  $E^2$  and is plotted as plotted in Figure 1.

Here, it can be seen that the half-power beamwidth of the antenna pattern in the horizontal plane is  $\sim 7^\circ$ , which is much narrower than the

horizontal beamwidth of the individual antennas forming the array. Hence, the total power transmitted by the 16 antennas is concentrated into a much smaller azimuthal angle and, therefore, the power density of radiated signals near  $\theta=0$  is significantly enhanced.

### Time Delay Steering

The principals that have just been described are equally applicable to the fringe pattern produced by illuminating an optical grating. In that case, one observes a central white light fringe bordered on either side by several spread visible light spectra. The white light spectrum is  $m=0$  and displays no wavelength dependence, whereas the bordering spectra are  $m=\pm 1, \pm 2$ , etc, and appear as grating spectra because the response for  $\theta \neq 0$  is wavelength dependent. The radiation pattern shown in Figure 1 is also an  $m=0$  response. The location of the peak remains at  $\theta=0$  for all frequencies, since the distance from the antennas to a remote target is the same for each antenna. The width of the peak will increase with increasing wavelength, since the spectral width is dependent on the ratio of the wavelength to the length of the array.

Now let us consider how we might rotate the  $m=0$  spectral peak to an azimuth angle other than zero degrees. Figure 2 shows a schematic of four RF signal sources that are oscillating in phase and connected to four antennas through cables of length  $L1, 2L1, 3L1$ , and  $4L1$ . The dotted lines represent propagation from the antennas in one particular direction. The radiated signals no longer reinforce in the  $\theta=0$  direction, since they leave the antennas with different phases. However, in the direction drawn they do reinforce. In this special direction, the total path length from each RF source to a distant target is the same.

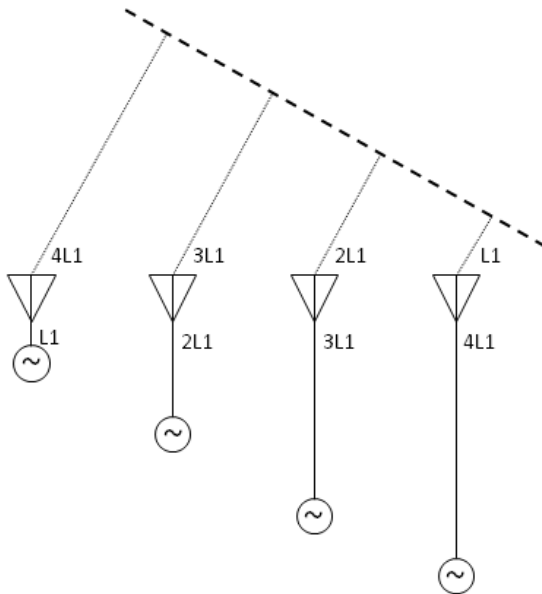


Figure 2

In the figure the dashed line represents a plane wave surface that is normal to the dotted lines. In each case, the distance between one of the sources and the dashed line is equal to  $5L1$ . If the signals are in phase along the dashed line, they will remain in phase at any greater distance. In effect, the varying cable lengths have rotated the  $m=0$  white light fringe into a new direction that is determined by the increase in cable length between neighboring antennas. This technique is known as “time delay steering” and it rotates the azimuth angle of the  $m=0$  fringe by

$$\theta = \sin^{-1}(L1/d). \tag{2}$$

In effect, the varying cable lengths have rotated the  $m=0$  white light fringe into a new direction that is determined by the increase in cable length between neighboring antennas. This technique is known as “time delay steering” and it rotates the azimuth angle of the  $m=0$  fringe by

Since the path length between each of the RF sources and the scattering region is the same, the signals from the four transmitters will always undergo constructive interference in the direction identified by (2). This result is frequency independent and the primary reason why “time delay steering” is very well suited for broadband radar systems.

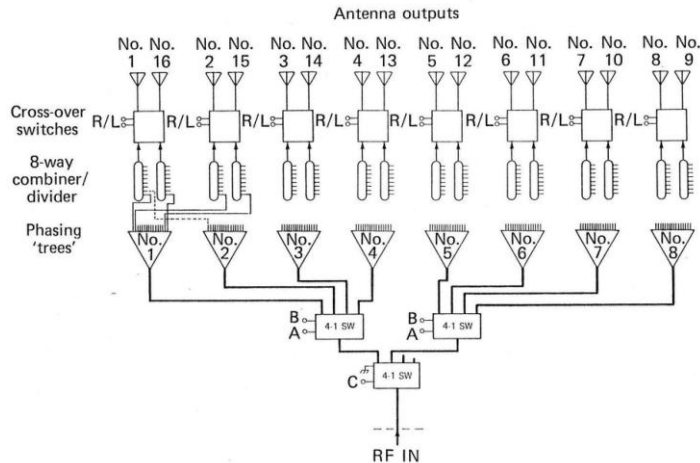


Figure 3 Schematic of phasing matrix used in original Goose Bay radar. This device established a progressive time delay across the antenna array on transmission and reformed the beam on reception. The 4-1 switches select one of eight possible branching networks and (phasing ‘trees’). Each ‘tree’ consists of power dividers and delay lines that produce a specific progressive time delay across the 16 outputs of the ‘tree’ and correspond to one of eight possible beam directions on either side of the array normal. The crossover switches determine whether this beam is directed to the right or left of the array normal. On reception, the process is reversed and the matrix reinforces only those signals from the selected beam direction.

Time delay steering is the technique that was used on the original Goose Bay radar constructed in 1983. At that time, cable segments were used to provide the time delays. These segments were arranged in networks identified as phasing ‘trees’ in Figure 3, which was taken from *Greenwald et al.*[1985]. The operation of the matrix is described briefly in the figure caption. Each of the phasing trees provides all of the cable delays for one beam direction. The phasing tree is selected by the least significant 3 bits of the beam number. The most significant bit controls the cross-over switches and determines whether the beam is directed to the right or left of the array normal direction. The beams have an azimuthal spacing of  $3.24^\circ$  and the central two beams are spaced  $\pm 1.62^\circ$  from the array normal direction.

Due to the significant amount of cable used in the phasing matrix, the container holding the matrix cables and components took up about  $1\text{ m}^3$  of space and provided a convenient seat. At the beginning of the SuperDARN era in the early 1990s, the French contingent of the SuperDARN community developed a compact version of the original design that replaced the cable segments with capacitive delay lines and reduced the size of the phasing matrix to eight PCBs. Each PCB contained the capacitive delay lines for beam selection on one pair of antennas and control circuitry for switching beams. Each PCB was explicitly constructed for one pair of antennas, e.g. (1,16). The beam spacing on the SuperDARN era PCBs was identical to that on the original Goose Bay radar. The  $3.24^\circ$  spacing provided continuous, or near continuous, coverage over a  $52^\circ$  azimuth sector utilizing 16 beams.

In general, the original and SuperDARN-era phasing matrices work well. They enabled the radars to scan large regions of the high latitude ionosphere using a wide range of frequencies

with relatively little effort. They enabled the radars to provide consistent data sets that could be easily combined to yield global-scale observations of the high-latitude ionosphere. However, they also had some shortcomings. The most serious shortcoming was that the both the cable segments and the capacitive delay lines were lossy circuit elements and the losses became greater as the cable lengths and time delays increased. Thus, the beams that were directed the furthest from the array normal direction were impacted most by these losses and the losses were distributed in an asymmetrical manner across the array. Some mitigation was possible for the transmitted signals since the levels of the rf drive signals were adjusted with automatic gain control circuitry in the transmitter units. However, no corrections were possible for the received signals. Another shortcoming of these time delay phasing matrices is that they were relatively inflexible. They are designed and constructed to produce 16 beams with  $3.24^\circ$  spacing that were symmetrically distributed about the array normal direction. They also required an antenna spacing of 15.24m. If you wanted to rotate these beams into slightly different directions, you could do it by adding a set of auxiliary set of cables between the transmitters and antenna feed cables. However, if you wanted to change the angles between the beams, you would have to build a new phasing matrix with different capacitive delay lines or a new antenna array with different spacing between antennas (see (2)).

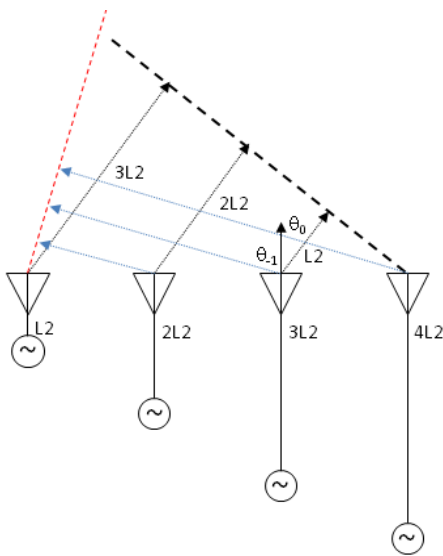


Figure 4. Modified version of Figure 2 showing both the  $m=0$  lobe and the  $m=-1$  grating side lobe. In this case all of the phase paths for the  $m=0$  mode have a length of  $4L2$ . The phase path lengths of the  $m=-1$  mode are all different, but they can still produce a lobe maximum (See Equation (3)).

Finally, there was another issue that is inherent to all phased-array antennas if the spacing between antennas becomes too large. If you steer the  $m=0$  fringe away from the array normal direction, you will concurrently steer either the  $m=1$  or the  $m=-1$  grating spectrum toward the array normal direction. At higher frequencies, the grating side lobe can move into the normal field of view covered by a SuperDARN radar scan. When this happens, the transmitted signal will be directed into two different directions with comparable levels of power and backscattered signals may be received from one or both directions. SuperDARN analysis routines assume that the backscattered power is coming from the  $m=0$  lobe, but the backscatter returns could be coming from a very different direction and have a substantially different Doppler shift from

that which would be associated with backscatter from the  $m=0$  lobe. These problems can be mitigated by knowing the frequencies that might be capable of producing grating sidelobe

backscatter and by choosing an antenna spacing that was less likely to produce grating sidelobe backscatter.

Figure 4 displays the  $m=-1$  grating sidelobe for a transmitted signal with wavelength  $\lambda$  given that the lag between each transmitter and its antenna increases as  $L2$ ,  $2L2$ ,  $3L2$ , and  $4L2$ . The red dashed line represents a constant phase surface emerging from the antennas. While the path lengths of transmission from the antennas to the red dashed phase surface are clearly different, there can still be constructive interference of the transmissions in the direction of the blue dotted arrows, if the path difference between each pair of adjacent antennas is equal to the wavelength  $\lambda$ . The angle  $\theta_{-1}$  for which this occurs is given by

$$\theta_{-1} = -\sin^{-1}((\lambda - L2)/d). \quad (3)$$

Several features of the grating sidelobe can be seen from (3). First, a grating sidelobe can only be formed if  $|(\lambda - L2)/d| \leq 1$ . Secondly, higher frequency transmissions have shorter wavelengths and therefore are more likely to produce grating sidelobes. If we assume a radar operating frequency of 16.67 MHz ( $\lambda=18\text{m}$ ) and  $L2=6.3\text{m}$ , then the  $m=0$  primary lobe forms at  $24.4^\circ$  and the  $m=-1$  grating lobe forms at  $-50.2^\circ$  for a SuperDARN radar with 15.24m antenna spacing, whereas the  $m=0$  primary lobe forms at  $-29.5^\circ$  and the  $m=-1$  grating lobe forms at  $-66.1^\circ$  for a radar with 12.8m antenna spacing. Note that the 15.24m antenna spacing has been used on most of the older SuperDARN radars as well as many of the newer radars, while the 12.8m spacing has been used on the mid-latitude SuperDARN radars constructed in North America using the twin-terminated folded dipole (TTFD) antennas. The smaller size of the TTFD antennas has allowed the closer antenna spacing which has reduced contamination from grating sidelobes at higher frequencies. The 12.8m spaced TTFD antennas have allowed the SuperDARN radar scan to be increased to as many as 24 beams with the traditional  $3.24^\circ$  beam separation. The azimuth sector scanned with these radars can be as large as  $78^\circ$ .

Recently, a third type of time-delay steering has been developed at the University of Alaska Fairbanks (UAF) for the new mid-latitude SuperDARN radars developed under the NSF Mid-Sized Infrastructure (MSI) Grant. The objective of the new design was to introduce more flexibility in the phasing matrix modules that would allow a much wider choice of beam spacing, antenna spacing and number of beams. All of the main array modules were essentially identical and could be used on at any antenna position. They were designed to allow any time delay in the range from 0.25 ns to 574 ns with an accuracy of  $\sim 0.25$  ns. Each board has 13 stages of delay selection, which allowed for some redundancy in delay selection. The boards also contain fixed and digitally-controlled attenuators to match the attenuations introduced by the capacitive delay lines and switches within the delay-line network. These boards have been fabricated at the University of Alaska, Fairbanks and by Scientific Instrumentation Limited in Saskatoon, Canada.

Once the boards have been fabricated, they need to be calibrated on a network analyzer for the specific mode of operation that is planned. For the MSI radars, they have been calibrated for

either 22 or 24 beam directions with an angular separation of 3.24 between beams. This process is automated and may require 1-2 days to complete. When the process is completed, the optimal set of delay and attenuator switch settings is burned into EEPROMs on each board. These settings are associated with beam numbers. When a particular beam is selected, the corresponding delay elements and RF attenuators are switched into the delay line network.

The attenuators maintain a uniform drive level across the array of antennas by attenuating the stronger signals, so there is no need for automatic gain control hardware to maintain uniform drive to the transmitter units. However, this has increased the losses in the phasing matrix, particularly due to the longer delays that are required for the 22-24 beam scans, so auxiliary amplifiers have been added to the transmitter side of the phasing matrix to increase the signal levels of the RF pulses powering the transmitters and the received signals from the antennas.



A photograph of a phasing card from one of the new MSI radars is shown in Figure 5. One of these cards is

Figure 5. Photo of phasing matrix card used in the new MSI radars. The right hand side of the card contains the 13 stage digital delay line. The left hand side contains digital control circuitry and EEPROM storage of delay and attenuation settings for available beam positions.

associated with each antenna of the main array and a slightly modified version is associated with each antenna of the interferometer array.

### *Phase Shift Steering*

To this point, we have only considered beam steering using time delay techniques. We have done so, because the time delay technique is frequency independent, a factor that simplifies the operation of the radars. However, when the number of antennas and the azimuth sector scanned become large all implementations of time-delay technology encounter difficulties due to inaccuracies and losses in the time delay elements and the many switches that may be required. An alternative approach is phase shift steering. We begin by discussing possible ways for it to be implemented and what its advantages are.

In Figure 2, we have seen that adding increasing lengths of cable between the transmitters and the antennas causes the  $m=0$  lobe of the antenna pattern to rotate away from the array normal direction. These lengths of cable were identified as multiples of some basic length  $L1$ . Each length of cable increases the time for the signal to propagate from the transmitter to the antenna therefore retards the phase that is reaching the antenna at any instant of time. Longer segments are retarded in phase by a greater amount and this ultimately causes the steering to occur. The phase retardation,  $\varphi$ , is proportional to the electrical length of the inserted cable segment, so if we have a segment of length  $nL1$ , the phase retardation is

$$\varphi=2\pi nL1/\lambda \quad (4)$$

and the difference in retardation between each pair of antennas is

$$\varphi=2\pi L1/\lambda \quad (5)$$

For the SuperDARN radars, the spacing of the antennas and the operating frequencies are such that  $\varphi$  will always lie between  $-\pi$  and  $\pi$ . If the shorter cable length is attached to the left hand antenna of the pair as it is in Figure 2, then  $\varphi$  is positive and the beam will rotated clockwise of the array normal direction. If the shorter cable length is attached to the right hand antenna, then  $\varphi$  is negative and the beam is rotated counterclockwise of the array normal. From (2), we see that  $L1=d\sin(\theta)$ . Making this substitution in (5) and solving for  $\theta$ , we obtain

$$\theta=\sin^{-1}(\varphi\lambda/2\pi d) \quad (6)$$

Equation (6) is the phase shifting counterpart to (2). If, for simplicity, we assume that the antennas in the array have a spacing of  $\lambda/2$ , then the rotation of the beam is  $\theta=\sin^{-1}(\varphi/\pi)$ . If we further assume that  $\varphi=\pi/2$ , or, equivalently that the phase shift is  $\lambda/4$ , then we see that the beam is formed at  $\theta= \sin^{-1}(1/2)=30^\circ$ . Alternatively, if we substitute  $L1=\lambda/4$  and  $d=\lambda/2$  into (2), we obtain  $\theta= \sin^{-1}(1/2)=30^\circ$ . Thus, the two approaches give the same result.

However, there is a difference between (2) and (6). If we set the cable length between the left-most transmitter and antenna of the array to zero length and increase the length of all subsequent cable segments to the right of this antenna by  $L1/\text{antenna}$ , then the length of the cable segments for a very long array can increase indefinitely. In contrast, if we set the phase of the left-most transmitter to zero and decrease the phase of all subsequent transmitters to the right of this transmitter by the value  $\varphi/\text{antenna}$ , the values do not increase continuously since  $\varphi$  is a cyclical quantity modulo  $2\pi$ .

Table 1 shows three methods involving cable segments or phase shifts that will produce a beam at  $\theta=30^\circ$ . We have assumed the simplified parameters identified in the preceding two paragraphs.

Table 1. Cable Lengths and Phase Shifts for Beam at  $\theta=30^\circ$  (8 Antenna Array)

Antenna #	1	2	3	4	5	6	7	8
Cable Length	0	6.4m	12.8m	19.2m	25.6m	32m	38.4m	44.8m
Phase Shift	0	$-\pi/2$	$-\pi$	$-3\pi/2$	0	$-\pi/2$	$-\pi$	$-3\pi/2$
Cable Residual	0	$\lambda/4$	$\lambda/2$	$3\lambda/4$	0	$\lambda/4$	$\lambda/2$	$3\lambda/4$

In this example, we assume the radar to be a U.S. mid-latitude SuperDARN radar with antenna separation of 12.8m. We know from (2) that the cable segments must be multiples of 6.4m in order to direct the beam to  $\theta=30^\circ$ . The second row of Table 1 shows the lengths of these segments for an 8 antenna array and we see that the cable segments are quite long. For a 16 antenna array, the lengths of the longest cables would more than double. We should note that a radar with the indicted cable segments or with capacitive delay lines having the same time delays, would produce a beam at  $30^\circ$  at all radar operating frequencies.

The third row of Table 1 shows a series of phase shifts that could be applied to transmitters 1-8. These values are obtained from (6) by requiring the argument of the arcsine function to be 0.5 and assuming that the  $\lambda=2d$ . The values in the third row are multiples of the phase shift of Antenna 2, but invoking the  $2\pi$  cyclical nature of the phase. These phase shifts only form a beam at  $\theta=30^\circ$  if the wavelength and operating frequency of the radar are 25.6m and 11.719 MHz.

Finally consider the cable lengths given in the fourth row of Table 1. These values were obtained by identifying cable lengths that are consistent with the phases of third row assuming that  $\lambda$  is the wavelength derived for the third row. Thus, a cable length of  $\lambda/4$ , should produce a phase delay of  $\pi/2$ , etc. It can also be seen that the cable residuals identified in Row 4 are equal to those in Row 2 for the first four antennas. The cables lengths for antennas 5-8 can be express as a wavelength of 25.6m plus a residual of 0,  $\lambda/4$ ,  $\lambda/2$ , and  $3\lambda/4$ , respectively. It can be concluded that all three of these rows are totally consistent, if Rows 3 and 4 are only used for a radar operating frequency of 11.719 MHz.

These results may be summarized as follows:

Time delay phasing beam steering can be used over a wide range of frequencies, but technical difficulties arise when the time delays become excessively long. These difficulties impact the performance of the phasing matrix and its long term reliability.

Phase shift steering either by direct phase control or using time delay residuals can provide reliable and accurate steering, but must be recalculated if the frequency of operation changes by more than a few percent. The reduction in technical difficulties results from the phase shifts being limited to a range of  $2\pi$  and the time delays being limited to the propagation time over a distance of one wavelength.

The initial implementation of phase shift steering took place in 2005 in association with the development of the first mid-latitude SuperDARN radar at Wallops Island, VA. This radar was the first to utilize Twin-Terminated Folded-Dipole (TTFD) antennas and, because of space limitations at the Wallops site, had an antenna spacing of 12.8m. The design of the phasing matrix, receiver and transmitter drivers were largely analog in nature and relied significantly on commercially available electronic modules. In this document, we concentrate primarily on the phasing aspects of the design and how they were implemented. The analog electronics for the Wallops radar, aside from the transmitter units, were largely implemented on five rack-mountable aluminum plates. The plates were identified as the:

- 50.625 MHz Phase Shifter: This plate uses the signals from the PTS-160 Frequency synthesizers to produce the various frequencies that were needed by the radar. It also contains an 8-bit phase shifter operating at 50.625 MHz to produce the basic phase shift,  $\phi$ , that was required for phase shift steering. The 8 control bits come from the digital interface box (BAS box). It was downloaded to the BAS box from the QNX computer into the 8-bit register that had originally been reserved for beam number and antenna number. The ROS software has been modified to offer either of these options. The accuracy of the phase selected is  $\sim\pm 0.75^\circ$ .
- 40.625 MHz Phase Generator: This plate produces all of the phase shifts needed to steer the main antenna array and the interferometer array. There are currently 15 stages to the generator, which is sufficient to drive a 16-antenna main array and up to 16-antennas in an interferometer array. Currently, only four of the interferometer outputs are used. The response of the phase generator is effectively instantaneous. Once the input phase  $\phi$  has been changed, all of the output phases have responded within a few microseconds.
- Tx Pulse Generator: This plate applies the appropriate phase to the transmitter drive pulse going to each of the transmitters/antennas.
- Rx Beam Former: This plate removes the differential phase from the signals coming from each of the main-array antennas/transmitters. Unlike delay line steering where a single matrix provides a two way path, a separate electronic path is required to remove the phase differentials.
- I/F Beam Former and Rx Front End: This plate forms the beam for the four antennas of the interferometer array and completes the analog amplification and filtering for the received signals from both the main and interferometer arrays. Since the beam forming process is the same as it is in the Rx Beam Former, we shall not discuss this plate further in this document.

The 50.625 MHz phase shifter board is only relevant to the current discussion in that it provides two signals at 50.625 MHz and +22 dBm that differ in phase by  $\phi$  radians. The delays in the phase shifter are produced by lengths of cable and sum to slightly less than one wavelength at 50.625 MHz. The total length of cable used is less than 4 m and introduces no loss in the signal level. The board also provides a 40.625 MHz signal at a level of +10 dBm. These signals are the inputs that are required by the 40.625 MHz Phase Generator plate.

A schematic of the 40.625 MHz Phase Generator Plate is shown in Figure 6. Note that a portion

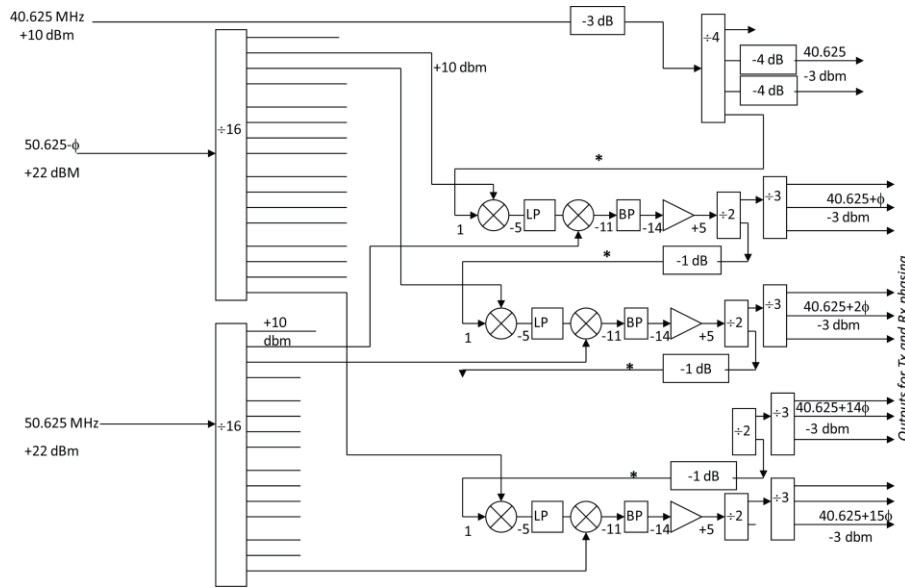


Figure 6. Schematic of 40.625 MHz phase generator board used at the Wallops SuperDARN radar site. Note that the schematic only shows the phasing outputs for the first three and final two transmitters/antennas of the array. The input 40.625 MHz signal is the reference signal for the phasing. Each stage of the generator takes the output from the previous stage and adds  $\phi$  radians.

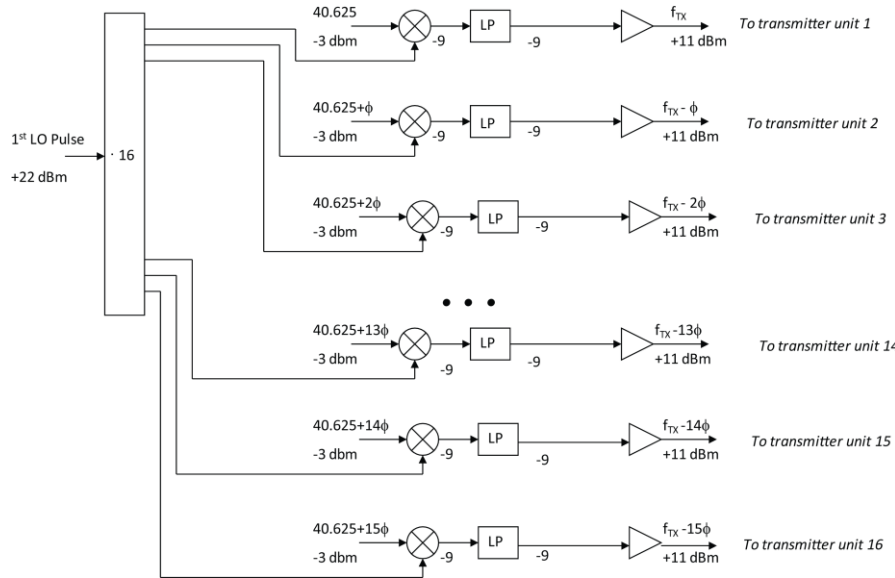


Figure 7. Schematic of Tx pulse generator board.

of the incident 40.625 MHz input signal is passed on to the first mixer chain where it is downconverted to 10 MHz and has a phase shift of  $\phi$  added to the signal. The second mixer upconverts the signal back to 40.625 MHz while retaining the phase shift that was added. The signal is filtered with a relatively narrow-band 4 MHz filter to remove unwanted mixing products and amplified to bring the signals levels at the outputs of the 3-port dividers to the attenuated outputs of the initial 4-port divider. The lengths of the cables feeding back to the next level of mixers can be altered slightly to remove slight phase anomalies and changing the value of the 1 dB attenuators can remove slight power anomalies. It should be noted that in addition to the phase  $\phi$  that is introduced by the first mixer in each stage of the generator there are additional phase delays due to the cables between stages and within each stage. These delays can all be accounted for by setting  $\phi$  to zero and adjusting the length of one of the 50.625 MHz input signals, so that all outputs overlap. Once the phase generator is properly adjusted it provides a set of properly phased 40.625 MHz signals that can be used for both transmission and reception. The outputs from the 40.625 MHz phase generator

of the incident 40.625 MHz input signal is passed on to the first mixer chain where it is downconverted to 10 MHz and has a phase shift of  $\phi$  added to the signal. The second mixer upconverts the signal back to 40.625 MHz while retaining the phase shift that was added. The signal is filtered with a relatively narrow-band 4 MHz filter to remove unwanted mixing products and amplified to bring the signals levels at the outputs of the 3-port dividers to the attenuated outputs of the initial 4-port divider. The lengths of the cables feeding back to the next level of mixers can be altered slightly to remove slight phase anomalies and changing the value of the 1 dB attenuators can remove slight power anomalies. It should be noted that in addition to the phase  $\phi$  that is introduced by the first mixer in each

go to both the Tx Pulse Generator and the Rx Beam Former. Some outputs also go to the I/F Beam Former and Rx Front End plate.

Figure 7 shows a schematic of how the HF drive pulses are created in the TX Pulse Generator. The inputs to this plate are pulsed 22 dBm transmissions at the 1<sup>st</sup> LO frequency and one set of -3dBm phase-delayed signals from the 40.625 MHz Phase Generator. The mixers and low-pass filters down-convert these inputs to pulse transmissions at the HF Tx frequency. All of the Tx drive pulses are of approximately equal amplitude and each of the Tx drive pulses acquires the correct phase delay to steer the transmitted radar signal into the proper beam direction.

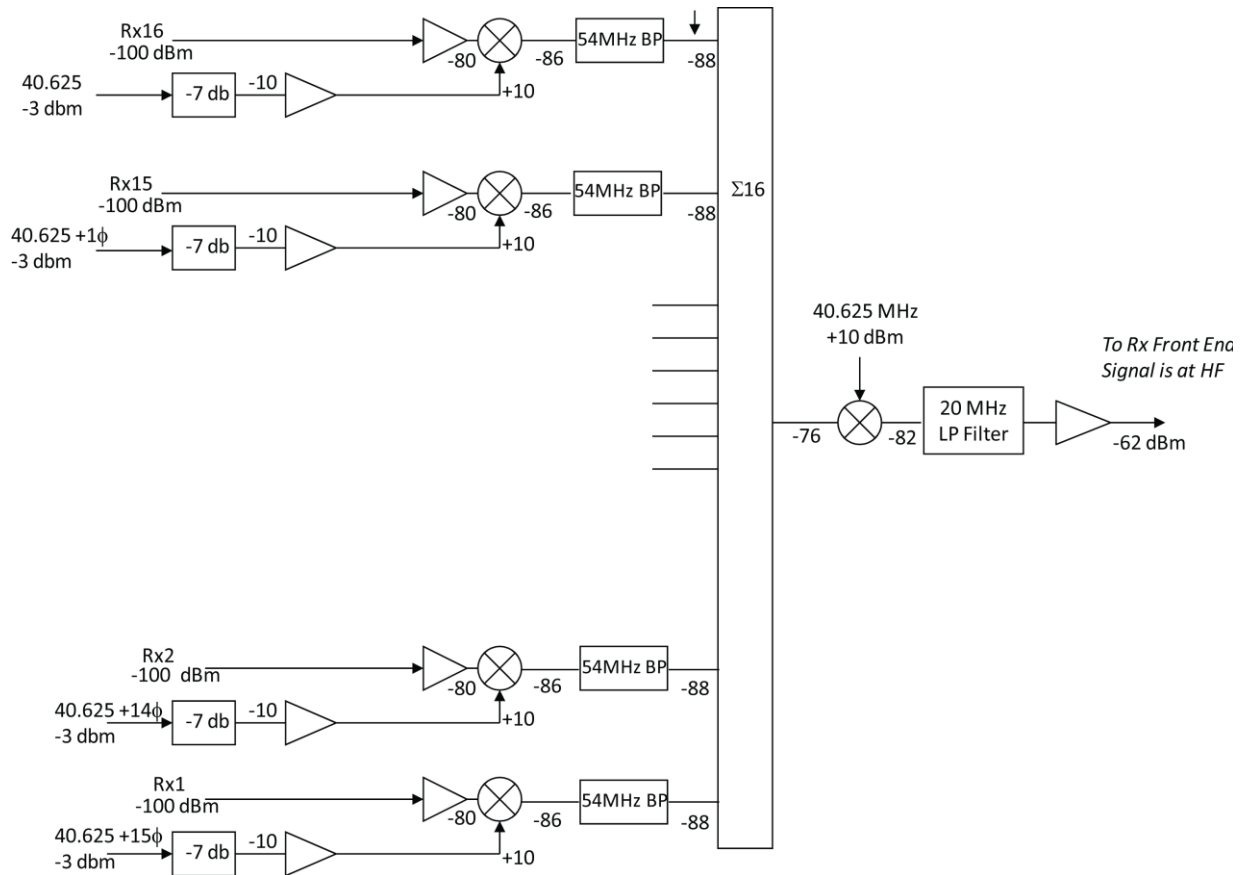


Figure 8. Schematic of Rx Beam Former

Figure 8 shows a similar schematic of how the signals received on the main antenna array are formed into a beam. If we assume that we are observing a signal coming from a direction that is clockwise of the array normal direction, than that signal will arrive first on the most eastward antenna and will reach the more westward antennas at progressively later times. Stated another way, the phase of the signal reaching each antenna at any instant of time will decrease by  $\phi$  per antenna as we move from the most eastward to the most westward antenna of the array. To remove these differences the phase of the 40.625 MHz reference signal reaching each mixer must increase by  $\phi$  per antenna as we move from the most eastward to the most westward antenna. This can be accomplished if the reference signals are attached to the antennas in reverse order as shown in Figure 8. Once the phase differences are removed the signal from the 16

antennas are summed coherently with a 16-port combiner. Finally the signal is down-converted to an HF frequency and passed to the receiver analog front-end where it undergoes additional amplification and filtering.

It can be seen in Figure 8 that the signal exits the Rx Beam Former as an HF signal with an apparent -3dB bandwidth of 20+ MHz. Actually, the bandwidth of the output signal is closer to 10 MHz since it is determined by the bandwidth of the 54MHz filters prior to the combiner. This approach was used so the electronics through the Rx Beam Former were the same for radars processing the received signal as an HF signal and those processing the received signals at an intermediate frequency in the VHF band. It now appears that if the signal were to be processed as an intermediate frequency, it would have been better to exit the Rx Beam Former as a VHF signal and omit the final three circuit components shown in Figure 8.

In summary, the Wallops phasing matrix functions very differently from the time delay phasing matrices that have traditionally been used with SuperDARN radars, but operationally it is almost as simple to use. With a traditional time-delay phasing matrix, one selects a beam number to use and the software selects the appropriate switches on the phasing cards. These cards continue to be used, independent of the frequency of operation, until a different beam number is selected. With the Wallops phasing matrix, one also selects a beam number to use, but the software calculates the phase shift  $\phi$  that is required to point in this direction. This value is output to the 50.625 MHz phase shifter, which provides a new phase shift to the 40.625 MHz Phase Generator. The radar immediately points to the new beam direction making minor adjustments as the new clear frequency is determined. It remains in that direction throughout the integration period and switches when the next beam direction is output.

It can be seen that there is very little difference in operation between traditional time-delay beam steering and phase steering. The only addition is a small and nearly instantaneous adjustment of the pointing direction when the clear frequency is selected. In return for this bit of extra effort, phase-shift steering allows the radar to be scanned over more beams and a wider azimuth sector than does the traditional time-delay phasing matrix which is only capable of creating 16 beams in its current implementation. Note that the time-delay phasing matrix developed at the University of Alaska/Fairbanks is capable of looking over a wider azimuth sector and many more beam directions, so the difference in capability is not due to time delay versus phasing shift steering, but rather how the particular technique was implemented. The original antenna configuration could only be scanned over 52° without introducing serious grating sidelobes. Given the nominal beamwidth of each lobe over most of the frequency range used, it was only necessary to have 16 beams.

There are two new developments to the phase shift steering implementation that was shown in Figures 6-8. The first involved a consolidation of repetitive groupings of RF components onto PCBs that are mounted on the various plates in metal cases. Examples of where this was done include the repetitive strings of mixers, filters and amplifiers that can be observed in Figures 6-8. Consolidating the components onto a PCB led to significant cost savings and a much neater layout on the various metal plates. This development has been integrated into several of the Canadian SuperDARN and PolarDARN radars, the mid-latitude SuperDARN radar in

Blackstone , VA, and an Italian SuperDARN radar that will be installed at Concordia Base in Antarctica at the end of 2012.

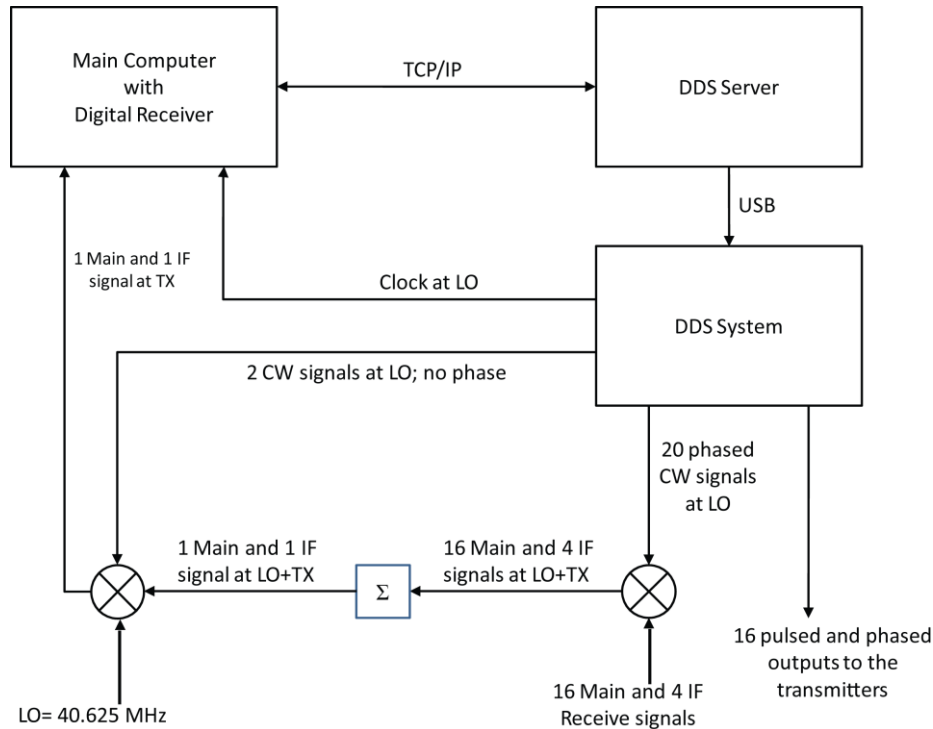


Figure 9. Phase-shift steered phasing matrix utilizing Direct Digital Synthesizer technology developed at the University of Saskatchewan.

The second development involves a further innovation to the phase shift steering implementation shown in Figures 6-8 by the Canadian SuperDARN group at the University of Saskatchewan. In the Canadian design (See Figure 9), the timing computer that is used at many SuperDARN radar sites is replaced by the DDS Server. This server receives operating parameters from the main radar computer via TCP/IP and calculates the timing-sequence, frequency and phase parameters that are needed to steer the radar beam and output the pulse transmissions for the next integration period. These parameters are transferred from the DDS Server to the PIC18F4550 microcontroller in the DDS System (See Figure 10). The microcontroller performs several tasks. First, it outputs the necessary frequency and phase information to each of the AD9959 Direct Digital Synthesizers (DDSs). This is done via the Chip Select and Serial Peripheral Interface (SPI) control lines shown in Figure 10 and the information is held in intermediate buffers. Each of the DDSs is capable of providing four output frequencies at specified phases. These signals may either be continuous (CW) or amplitude modulated with controllable rise and fall times. Next, the microcontroller creates a timing sequence using internal timers that modulate the pulsed transmissions (Pulse Control) from the radar. When all operating parameters have been fully specified, each I/O update request from the main computer to the PIC18F4550 via the DDS Server transfers the operating parameters into working registers of the DDSs and triggers a new

sequence of transmitted pulses. The backscatter returns are ultimately sampled by a digital receiver in the main computer where they are processed.

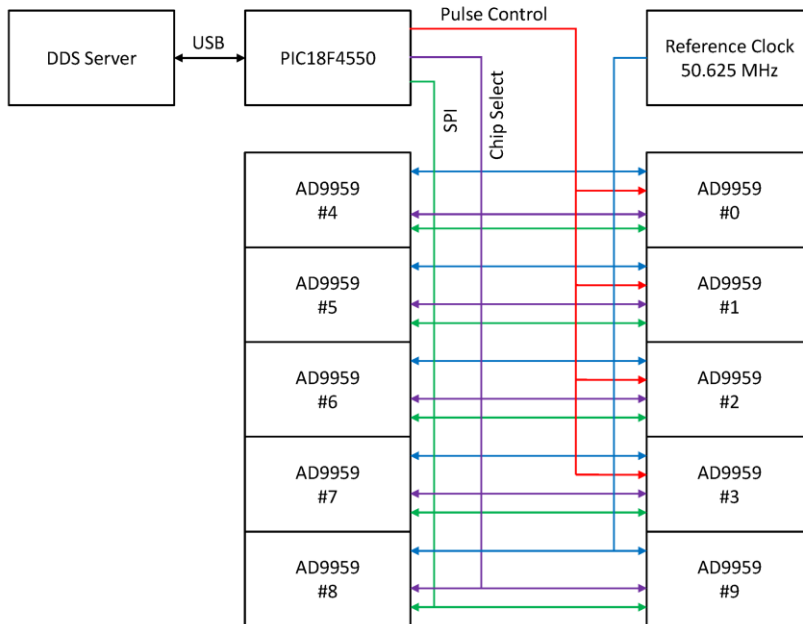


Figure 10. Detailed view of DDS Server and DDS System shown in Figure 9.

In the Canadian design, all but one of the PTS 160 Synthesizers that have been used on SuperDARN radars since the 1980s, the 50.625 MHz phase shifter plate, and the analog 40.625 MHz phase generator plate have been replaced by DDSs and a microcontroller. The remaining frequency synthesizer is used as a frequency reference for the DDSs and as a clock for the digital receiver. Since the HF transmitter pulses are produced directly by

the DDSs, the Tx pulse generator plate shown in Figure 7 is also unnecessary and has been eliminated. The mixers and summer shown in the lower left corner of Figure 9 represent the Rx Beam Former and the hardware shown in Figure 8 is still used as is equivalent hardware for beam forming of the interferometer array returns.

The first Canadian DDS-based radar has been operating from Inuvik, NT Canada since December 2010 and has performed reliably in a harsh environment and provided a significant amount of high quality data. The process of setting up a DDS-based radar with phase shift steering is more complex than that required for the analog equivalent. Instead of a single  $\phi$  input, a distinct phase must be sent to each of the DDS channels that produce a pulsed Tx signals going to a transmitter/antenna pair and on reception a distinct phase must be sent to each DDS channel that provides a local oscillator signal for the Rx Beam Former (note that this board is still being used). Each time the frequency or beam number is changed all of these phases must be recalculated and resent to the appropriate DDS units. While this is a more complex process, potential performance improvements resulting from usage of an accurately controlled digital system may make the effort worthwhile.

A second implementation of DDS beam steering on a SuperDARN radar is under development at La Trobe University near Melbourne, Australia. This radar will be installed at mid-latitude near Adelaide in southern Australia. At the present time, full details on the status of the development are not available.

*Summary:* This completes the review of beam-steering techniques that have been used in association with the SuperDARN radar network. Time delay techniques have the advantage of

operational simplicity. With this approach, the ordinal number of the beam is input and nothing more is done until the direction of the beam is changed. Unfortunately, this approach has always had technical challenges due to signal losses when using long cables and signal losses and delay inaccuracies when using capacitive delay lines. The technique is also subject to operational inflexibility. A given phasing matrix is associated with a given antenna spacing, if one wants to have a specific angular separation between beams. While this has generally been the case in the past, some of the newer radars have used different antenna separations and increased number of beams which would not have been possible with the original design of the time delay beam steering cards. It is, of course, possible with the newer design from the University of Alaska.

In contrast, the phase steering approach requires more attention to assure that the radar beam is pointing in the proper direction. The amount of attention varies from very little for the analog phase-steering approach shown in Figure 6, to fairly significant for the University of Saskatchewan DDS system shown in Figure 9. The difference lies in the fact that each DDS in the Canadian system must have its new phase calculated and output to the DDS, whenever the frequency of operation is changed by more than a few hundred kilohertz. This overhead may seem burdensome, but with advances in processing speed and technology, it may not remain an overwhelming concern.

One point is certain. The SuperDARN radar network has benefited greatly from its ability to scan over large spatial areas and produce data sets that cover large fractions of the Earth's mid and high-latitude ionosphere. This has opened up new insights on many physical processes occurring in the ionosphere, magnetosphere, and upper atmosphere and has helped advance our understanding of Earth's space environment.